Chinese Chemical Letters 35 (2024) 109140

Contents lists available at ScienceDirect

Chinese Chemical Letters

journal homepage: www.elsevier.com/locate/cclet

Recent advances on decomplexation mechanisms of heavy metal complexes in persulfate-based advanced oxidation processes

Shili Wang[a], Mamitiana Roger Razanajatovo[a], Xuedong Du[a,**], Shunli Wan[c], Xin He[b], Qiuming Peng[a], Qingrui Zhang[a,b,*]

[a] State Key Laboratory of Metastable Materials Science and Technology, Hebei Key Laboratory of Heavy Metal Deep-Remediation in Water and Resource Reuse, Yanshan University, Qinhuangdao 066004, China
[b] Hebei Key Laboratory of Agroecological Safetye Key Laboratory, Hebei University of Environmental Engineering, Qinhuangdao 066102, China
[c] College of Life & Environment Sciences, Huangshan University, Huangshan 245041, China

ARTICLE INFO

Article history:
Received 2 June 2023
Revised 3 September 2023
Accepted 21 September 2023
Available online 23 September 2023

Keywords:
Heavy metal complexes
Persulfate
Advanced oxidation processes
Decomplexation mechanisms
Electron and energy transfer

ABSTRACT

In some industrial wastewater, heavy metals combine with organic complexing agents to form heavy metal complexes (HMCs). These HMCs can be difficult to decompose and remove through conventional techniques due to their higher stability than free heavy metal ions. In recent years, persulfate based advanced oxidation processes (PS-based AOPs) have been recognized as a viable technique for HMCs degradation. Nevertheless, a comprehensive and in-depth understanding of the relevant HMCs decomplexation mechanisms in PS-based AOPs is still lacking. This review delineates the current progress of HMCs decomplexation in PS-based AOPs. We discuss the distinctions between the two widely used oxidant types in PS-based AOPs techniques. Moreover, we summarize and highlight the decomplexation mechanisms based on electron and energy transfer, and degradation pathways of HMCs. We also emphasize the effects of environmental water constituents, namely pH, inorganic ions, and natural organic matter (NOM), on HMCs decomplexation. Ultimately, we identify the existing challenges and perspectives that will steer the direction of advancing PS-based AOPs to remove HMCs.

1. Introduction

With the rise of industrial activity, heavy metal pollution is a growing concern for the environment and human health [1,2]. Heavy metal contaminants are notorious for their indestructibility, contributing to their environmental persistence [3]. Additionally, heavy metals tend to bind with functional groups of complexing agents such as ethylenediaminetetraacetic acid (EDTA), nitrilotriacetic acid (NTA), and citric acid to form a heavy metal complex (HMCs), which are significantly more stable than free heavy metal ions and thus more hazardous to the aquatic environment and pose severe threats to public health [4,5]. HMCs are commonly found in wastewater from various industries, including electroplating, printing, textile, and curries [6]. Moreover, a number of techniques, including absorption, chemical precipitation, and ion exchange, have been developed to eliminate HMCs from wastewater [7]. Nevertheless, these methods are ineffective at removing HMCs due to their drawbacks, such as generating secondary pollution and new HMCs. Consequently, emerging technology, such as advanced oxidation processes (AOPs), has been proposed to extract and remove HMCs, due to their strong oxidation ability and high reactive oxygen species (ROS) production [8,9]. The ROS have the potential to decomplex HMCs, thereby releasing heavy metal ions, which is the most efficient way to remove HMCs [10].

In the past few years, AOPs such as Fenton-like oxidation and other combination technique have been applied to treat HMCs in wastewater [11,12]. Moreover, strong oxidants such as hydrogen peroxide (H_2O_2) are commonly used in AOPs to treat wastewater containing HMCs. However, H_2O_2 cannot dissociate HMCs on its own. To address this issue, H_2O_2 is widely used in conjunction with Fe(II) ions to produce hydroxyl radical ($^{\bullet}OH$) *via* the Fenton reaction [13,14]. In contrast, when Fe(II) activates H_2O_2, Fe(II) transforms into Fe(III), resulting in the formation of Fe sludge. This sludge formation can potentially exacerbate the problem of heavy metal contamination [15], because the heavy metal sludge is hazardous and difficult to dispose of properly. Therefore, limiting the efficacy of the Fenton reaction treatment of HMCs [16]. Although it is ideal to address the oxidation of HMCs through

* Corresponding author at: State Key Laboratory of Metastable Materials Science and Technology, Hebei Key Laboratory of Heavy Metal Deep-Remediation in Water and Resource Reuse, Yanshan University, Qinhuangdao 066004, China.
** Corresponding author.
E-mail addresses: duxd@ysu.edu.cn (X. Du), zhangqr@ysu.edu.cn (Q. Zhang).

https://doi.org/10.1016/j.cclet.2023.109140
1001-8417/

Table 1
Differences in characteristics between peroxymonosulfate (PMS) and peroxydisulfate (PDS).

Characteristics	PMS	PDS
Physical features	A free-flowing white granular powder soluble in water	White crystal, soluble in water, water-absorbing quality
The position of the O–O band	Unilateral position	Central position
The energy of cleavage of the O–O band	377 kJ/mol	92 kJ/mol
The redox potential	1.82 V	2.01 V
Specific types	Potassium peroxymonosulfate complex salt	Potassium persulfate and ammonium persulfate

ozone (O_3) without causing secondary pollution, the high cost of generating O_3 and the lack of efficient control over the amount of O_3 utilized pose significant challenges [17]. For these reasons, developing a novel technique to address the current problem is necessary. Persulfate (PS) based-AOPs have been considered the most promising technology for removing HMCs from wastewater due to the following benefits: (1) In PS-based AOPs could generate more sulfate radical ($SO_4^{\bullet-}$) than $^{\bullet}OH$ [18]; (2) The redox potential of $SO_4^{\bullet-}$ (2.6–3.1 V) is greater than that of $^{\bullet}OH$ (1.8–2.7 V), allowing for effective oxidation over a wide pH range [19]; (3) $SO_4^{\bullet-}$ have longer life span (around 30–40 μs) than other free radicals such as $^{\bullet}OH$ (only 1.0 μs), leading to the adequate performance of PS-based AOPs for pollutant removal [20]. Besides, PS is a more stable compound for storage and transportation than H_2O_2 [21].

Although several reviews on HMCs removal technologies have been reported in recent years [7,12], there are still significant gaps in our understanding. To the best of our knowledge, a critical review focusing on the decomplexation of HMCs using PS-based AOPs techniques, the decomplexation mechanisms, and pathways of HMCs, as well as the influence of the water environment constituents on the decomplexation process has not been published. Herein, the recent significant progress in HMCs decomplexation in PS-based AOPs is reviewed. The different types of oxidants used in PS-based AOPs techniques and their characteristics are discussed. Moreover, HMCs decomplexation mechanisms and pathways are emphasized. We also highlight the effects of water environment conditions such as pH, inorganic ions, and natural organic matter (NOM) on the HMCs' decomplexation process. The existing challenges and perspectives of using the PS-based AOPs technique are also discussed. We hope this review will offer valuable guidance for advancing PS- AOPs techniques for efficiently removing HMCs from wastewater.

2. Oxidant types in PS-based AOPs

There are two types of PS oxidants, namely peroxymonosulfate (PMS) and peroxydisulfate (PDS). Peroxymonosulfate (PMS) is a white, granular powder with free-flowing characteristics produced using peroxysulfuric acid (also known as Caro's acid). The PMS salt comprises three components: $KHSO_5$, $KHSO_4$, and K_2SO_4 [22]. On the other hand, PDS was produced with peroxydisulfuric acid. There are three forms of PDS: potassium PDS, ammonium PDS, and sodium PDS. Potassium PDS and sodium PDS are commonly used. However, ammonium PDS is less commonly used due to the readily evaporation of ammonium [23]. Although PMS and PDS are typically oxidants in PS-based AOPs, they differ significantly in their chemical composition, essential properties, and physical characteristics (Table 1). PDS has a symmetrical structure with the O–O bond situated in the center, while PMS does not and has the O–O bond located on one side [24]. Additionally, the required energy to break the peroxide bond varies between the two oxidants, in which PMS requires more energy than PDS [25]. These differences allow PMS and PDS to have different effects when being activated or removing contaminants. For instance, PMS can be activated by transition metals and metal compounds, whereas PDS tends to be activated through energy output, such as photolysis and pyrolysis [26]. Both PMS and PDS have oxidation properties that can directly oxidize pollutants, but it is difficult for PMS and PDS to directly attack HMCs. Instead, ROS plays a more significant role in degrading HMCs through PS-based AOPs [11]. Therefore, the activation of PS is crucial for the decomplexation of HMCs.

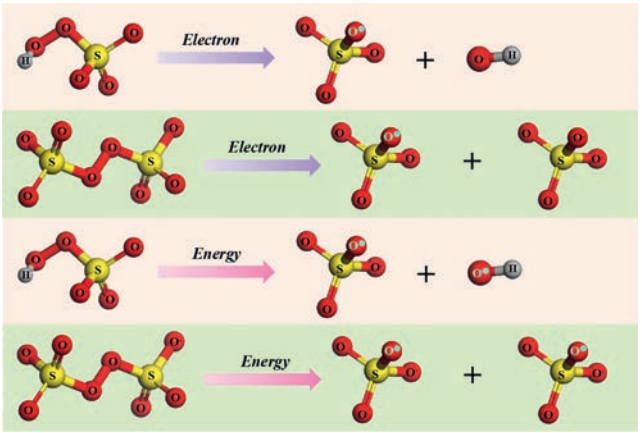

Fig. 1. Mechanisms of activated PMS and PDS by electron- and energy-transferring processes.

As shown in Fig. 1, PMS activation can be classified into two distinct types: electron-transferring and energy-transferring processes [27]. Typically, electrons donors include electricity and metal materials, while energy donors include UV lamps and heat. In the electron-transferring process, the external addition of one electron causes PMS to break down the peroxide bond, generating $SO_4^{\bullet-}$ and OH^-. Similarly, PDS is activated when it receives an electron, destroying the peroxide bond and producing $SO_4^{\bullet-}$ and SO_4^{2-} [28]. Using an electron-transfer activation process, the metal in the complex can activate PS to a small degree during HMCs treatment. Combining PS with other substances can enhance the activation and removal of metal complexes. In the energy-transferring process, PMS absorbs energy to produce $SO_4^{\bullet-}$ and $^{\bullet}OH$ during the energy-transfer process, whereas PDS generates only $SO_4^{\bullet-}$ [29]. Both methods activate PS, but their respective mechanisms are distinct. The two modes can be carefully selected for the desired results under various application conditions. This review did not thoroughly discuss the decomplexation mechanisms of HMCs in PS-based AOPs.

3. Decomplexation mechanisms

3.1. Self-catalyzed decomplexation

HMCs are formed when lone pair electrons in the ligand interact with the vacant orbitals in the heavy metal ions, transition metals such as Co(II), Fe(II), Cu(I), Ce(III), V(III), Mn(II), and Ni(II) are essential components for PS activation [30]. The HMCs' distinct structure allows them to activate PS and undergo self-breaking directly (Fig. 2). Co-EDTA, originating from the nuclear industry, was efficiently degraded in the presence of only PMS under acidic conditions (Table 2) [31]. The decomposed Co-EDTA released Co(II) ions that reacted with PMS, resulting in the formation of $SO_4^{\bullet-}$ (Eq. 1). This compound then reacted with H_2O to produce $^{\bullet}OH$ (Eq. 2) [32]. The PMS system was more suitable than the Fenton process due to its superior efficiency in decomplexing Co-EDTA with-

Table 2
Summary of the removal of heavy metal complexes (HMCs) in persulfate-based advanced oxidation processes (PS-based AOPs).

Activation methods	Heavy metal complexes/ Concentrations (mmol/L)	Conditions	Time (min)	Decomplexation efficiencies (%)	Heavy metal recovery (%)	Reactive species	Ref.
Self-catalysis							
Acid/Alkali	Co-EDTA/1.78	PMS = 142 mmo/L, pH 3.0	120	90.3	–	$SO_4^{\bullet-}$, $^{\bullet}OH$	[31]
Acid/Alkali	Cu-EDTA/0.1	PDS = 10 mmol/L, pH 2.0	90	98.9	–	$SO_4^{\bullet-}$, $^{\bullet}OH$, $^{\bullet}O_2^-$, $^1O_2$	[34]
Alkali	Ni-EDTA/0.03	PMS = 5 mmo/L, pH 11.0	60	93.2	–	$SO_3^{\bullet-}$, $^{\bullet}O_2^-$, $^1O_2$, Ni^{IV}	[37]
Electron-transferring processes							
Homogeneous catalysis	Cu-EDTA/0.1	PMS = 15 mmol/L, Co^{2+} = 1.0 mg/L, pH 3.0	120	98.2	–	$SO_4^{\bullet-}$, $^{\bullet}OH$	[40]
Heterogeneous catalysis	Cu-EDTA/0.47	PDS = 10 mmol/L, ZVI = 2 g/L, pH 5.0	60	77.2	–	$SO_4^{\bullet-}$, $^{\bullet}OH$	[47]
Heterogeneous catalysis	Cu-EDTA/3.14	PDS = 47.1 mmol/L, CuO = 2 g/L, pH 11	120	100	–	$SO_4^{\bullet-}$, $^{\bullet}OH$, $^{\bullet}O_2^-$	[50]
Heterogeneous catalysis	Cu-EDTA/0.01	PMS = 0.2 mmol/L, $Ti_3C_2T_X$ = 60 mg/L, pH 4.0	20	100	84	$SO_4^{\bullet-}$, $^{\bullet}OH$	[55]
Heterogeneous catalysis	Cu-EDTA/1.0	PDS = 4 mmol/L, Fe-MOF = 0.4 g/L, pH 3.0, J = 2.86 mA/cm^2	100	100	87.8	$SO_4^{\bullet-}$, $^{\bullet}OH$	[59]
Energy-transferring processes							
UV (254 nm)	Cu-EDTA/0.3	PDS = 18 mmol/L, Light intensity = 0.25 mW/cm^2, pH 6.0	90	100	–	$SO_4^{\bullet-}$, $^{\bullet}OH$	[65]
UV (254 nm)	Cu-EDTA/0.25	PDS = 2.5 mmol/L, Light intensity = 0.3 mW/cm^2, pH 4.0	40	60	–	–	[68]
Heat	Cu-EDTA/0.1	PDS = 20 mmol/L, T = 60 °C, FA = 10 mmol/L, pH 3.6	90	97.6	–	$SO_4^{\bullet-}$, $^{\bullet}OH$, $^1O_2$	[70]
Coupling electron- and energy-transferring processes							
Photo-electricity (UV, 254 nm)	Cu-EDTA/0.5	PDS = 10 mmol/L, J = 0.5 mA/cm^2, pH 3.0	60	93.1	92.7	$SO_4^{\bullet-}$, $^{\bullet}OH$	[77]
Non-thermal plasma	Cu-EDTA/0.5	PDS = 2 mmol/L, Applied voltage = 7.0 kV, pH 5.0	20	86	–	$SO_4^{\bullet-}$, $^{\bullet}OH$, $^{\bullet}O_2^-$, $^1O_2$	[82]

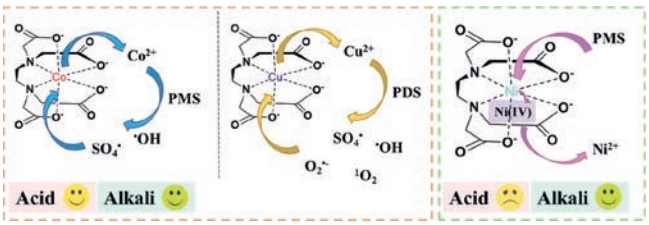

Fig. 2. Schematic of self-catalyzed decomplexation of HMCs.

out requiring additional catalyst dosages and in a shorter reaction time. This resulted in saved reagents and reduced costs. The highest efficiency occurred when the [PMS]/[Co-EDTA] molar ratio was approximately 80. However, this positive effect was relieved when the ratio exceeded certain levels, which could be attributed to the less reactive $SO_5^{\bullet-}$ species formed by scavenging $SO_4^{\bullet-}$ with HSO_5^- (Eq. 3) [33].

Wang and co-workers investigated the decomplexation of Cu-EDTA using autocatalytic PDS oxidation [34]. Cu-EDTA activated PDS, causing ROS to attack Cu-EDTA, leading to the release of Cu(II) ions and conversion to Cu-containing intermediates. Cu(II) ions and intermediate products further catalyzed PDS to produce more ROS, promoting Cu-complexes degradation. Electron paramagnetic resonance (EPR) detected significant levels of ROS for $SO_4^{\bullet-}$, $^{\bullet}OH$, and $^1O_2$ (Eq. 2 and Eqs. 4–8) [35]. The ratio of Cu to EDTA played a crucial role in the self-activation process. Excess Cu(II) ions aided in the decomplexation of Cu-EDTA, whereas excess EDTA inhibited it [36]. However, the removal of Ni-EDTA and Fe(III)-EDTA was less than 20% in the acidic self-catalyzed decomplexation, indicating that the direct activation of PS by HMCs was selective. The alkaline PMS process was a feasible approach for the self-decomplexation of Ni-EDTA [37]. In an alternative reaction pathway, PMS attacked Ni(II) rather than EDTA, resulting in the formation of an O=Ni(IV)-EDTA compound, which eventually self-decomplexed into Ni(III) hydroxides. Incorporating Ni(IV) species in this process provided a viable redox pathway that contributed significantly to the decomplexation. Ni-containing species also needed to be considered as well. Under alkaline conditions, Ni(II)-EDTA was mainly in the form of [HO–Ni(II)-EDTA]$^{3-}$. The unpaired electrons in the exposed Ni(II) sites were easily attacked by electrophilic PMS [38]. The Ni(IV) species served as the primary intermediate, and $^1O_2$ played an auxiliary role. Self-catalyzed decomplexation is a low-cost and convenient way that does not require catalysts, heat, light, and electricity. However, autocatalytic PS oxidation is constrained by the types of HMCs used, the metals-to-ligands ratio, and the pH of the solution. Consequently, it is necessary to strengthen the electron-transferring and energy-transferring processes.

$$Co^{2+} + HSO_5^- \rightarrow Co^{3+} + SO_4^{\bullet-} + OH^- \quad (1)$$

$$SO_4^{\bullet-} + H_2O \rightarrow SO_4^{2-} + {}^{\bullet}OH + H^+ \quad (2)$$

$$HSO_5^- + SO_4^{\bullet-} \rightarrow SO_5^{\bullet-} + SO_4^{2-} + H^+ \quad (3)$$

$$Cu^{2+} + S_2O_8^{2-} \rightarrow Cu^{3+} + SO_4^{\bullet-} + SO_4^{2-} \quad (4)$$

$$Cu^{3+} + S_2O_8^{2-} + 2H_2O \rightarrow Cu^{2+} + 2HSO_4^- + O_2^{\bullet-} + 2H^+ \quad (5)$$

$$Cu^{2+} + O_2^{\bullet-} \rightarrow Cu^+ + O_2 \quad (6)$$

$$Cu^+ + S_2O_8^{2-} \rightarrow Cu^{2+} + SO_4^{\bullet-} + SO_4^{2-} \quad (7)$$

$$^{\bullet}OH + O_2^{\bullet-} \rightarrow {}^1O_2 + OH^- \quad (8)$$

3.2. Enhanced decomplexation by electron-transferring process

ROS formation is vital for the enhanced decomplexation of HMCs in PS-based AOPs; selecting reduction catalysts is an essential step in the electron-transfer process [39]. For homogeneous processes, Co(II)/PMS system was the preferred choice for the degradation of Cu-EDTA, compared to Co(II)/PDS, Mn(II)/PMS(PDS), Ni(II)/PMS(PDS), Cr(III)/PMS(PDS), Fe(II)/PMS(PDS), Fe(III)/PMS(PDS), and Cu(II)/PMS(PDS) [40]. Despite the low Co(II) ions concentration at 10 ppb, significant quantities of Cu were released within 120 min. Co(II) ion has been shown to effectively activate PMS and promote ROS ($SO_4^{\bullet-}$ and $^{\bullet}OH$) production. Co(III) ion can act as an oxidant in its own right [41]. Moreover, it was discovered that replacing metal ions significantly affected the decomplexation efficiency of metal ion-catalyzed PS processes. Based on thermodynamic calculations and chromogenic experiments, EDTA and metal ion affinity sequences were determined as follows: Ni(II) > Co(II) ≈ Cd(II) > Mn(II) [42]. The oxidative performance of the Co(II)/PMS system was reduced following the substitution reaction between Co(II) and Mn-EDTA. Similarly, due to the strong interaction between Fe(III) and EDTA ($\log K_{Fe(III)\text{-}EDTA} = 25.2$), neither Fe(II)/$H_2O_2$ nor Fe(III)/H_2O_2 was able to efficiently decomplex Cu-EDTA [43]. Although the replacement reaction of Fe(III) and Cu-EDTA could release Cu(II) ions, Fe(III)-EDTA needed to be removed using specific methods, such as UV light coupled alkali precipitation [44].

The cooperation of metallic substances and HMCs in heterogeneous catalysis can enhance the activation of oxidants like H_2O_2 and PS [45]. Heterogeneous catalysis outperformed homogeneous catalysis regarding reaction time and HMCs removal efficiency [46]. For instance, a combination of zero-valent iron (ZVI) and PDS could be removed 77.2% Cu-EDTA within 60 min due to the ZVI's ability to slowly release Fe(II) ions for activation of PDS while producing Fe(III) ions to replace Cu(II) in the complex [47]. With the addition of ZVI to PDS treatment, the removal of TOC increased from 22.2% to 55.2%. Moreover, the concentration of dissolved Fe in the ZVI/PDS system was 6-fold higher than in the ZVI system. This indicates that the addition of PDS increased the concentration of dissolved Fe, which could improve the $SO_4^{\bullet-}$ yield (Eq. 9) [48]. On the other hand, in the presence of ZVI, the removal of Cu(II) decreased as the Cu(II)/EDTA ratio decreased, which is similar to the self-catalyzed decomplexation of Cu-EDTA/PDS, indicating that ZVI's surface passivation limited its reusability [49]. CuO exhibited persistent catalytic activity and exceptional reusability [50]. Moreover, the rate constant value of Cu(II) gradually increased from 0.033 min^{-1} (1st round) to 0.049 min^{-1} (24th round). When PDS has introduced alone, the removal of Cu(II) reached about 13.5% after 120 min, indicating insufficient oxidation capacity, whereas Cu(II) concentration was reduced by 57% using the alkali activation method. After adding CuO under alkaline conditions, the concentration of Cu in the solution changes insignificantly, indicating a limited adsorption capacity in this process. As shown in Fig. 3a, combining synergetic catalysis of PDS with CuO and Alkali resulted in the complete removal of Cu(II), implying that electron transfer between PDS and CuO/alkali was rapid, resulting in a high yield of $SO_4^{\bullet-}$ and $^{\bullet}OH$ [51]. $O_2^{\bullet-}$, $SO_4^{\bullet-}$, and $^{\bullet}OH$ were all equally important in this decomplexation process (Eq. 5). OH^- played a crucial role in the synergistic activation of PDS, as it could quickly neutralize the H^+ produced by the decomposition of PDS [52]. This neutralization promoted the cycle of Cu(II), Cu(III), and Cu(I), thereby enhancing the reusability and stability of CuO. The X-ray diffraction analysis revealed that the composition and structure of CuO particles remained unchanged throughout all 24 experimentation cycles. The gradual increase of CuO from 1.00 g to 3.12 g was advantageous for the decomplexation of Cu-EDTA.

In addition to traditional metallic elements and oxides, novel two-dimensional and three-dimensional materials, such as MXene and metal-organic frameworks (MOFs) [53,54], have been utilized in PS-based AOPs. MXene advocated for the self-degradation of the Cu-EDTA/PMS system [55]. The $Ti_3C_2T_x$/PMS process removed 100% of Cu-EDTA within 3 min, significantly faster than the $Ti_3C_2T_x$ processes (8%) and the PMS processes (5%). In the beginning, Ti(III) exposed to $Ti_3C_2T_x$ surface activated PMS (Eqs. 10 and 11) [56]. The uncoordinated Ti-O sites captured Cu(II) ions to form Ti_3C_{2-}O-Cu(II), as X-ray absorption near-edge spectroscopy and extended X-ray absorption fine structure demonstrated. Cu(II) was reduced to Cu(I) due to the reducibility of low-valent Ti and the short electron transfer distances [57]. As a result, incorporating Cu-EDTA into the $Ti_3C_2T_x$/PMS process resulted in a significant increase in PMS decomposition efficiency as well as the production of a large amount of $SO_4^{\bullet-}$ and $^{\bullet}OH$ (Fig. 3b). Additionally, Cu(II) ions could be absorbed by the negatively charged $Ti_3C_2T_x$, resulting in metal recovery. However, the increase in PMS concentration did not assist in Cu recovery. After the 5th cycle, the oxidation of $Ti_3C_2T_x$ reduced the adsorption sites, resulting in a sharp decline in recycling efficiency. For electroplating wastewater treatment, the removal efficiency of Cu(II) and the chemical oxygen demand were 82.2% and 30.0%, respectively. In addition, electrochemical (EC) methods can also assist in the reduction of high-valent metals [58]. Zhang *et al*. investigated the EC/Fe-MOF/PDS system for Cu-EDTA decomposition (Fig. 3c) [59]. The ratio of Fe(II) to Fe(III) in pristine Fe-MOF (0.003) was lower than in used Fe-MOF (0.121), indicating that the cathode promoted the production of more Fe(II). If the current were too high, a substantial amount of hydrogen gas would overflow from the cathode, reducing overall current efficiency [60]. According to X-ray photoelectron spectroscopy, Cu species were deposited on the surface of the used Fe-MOF, raising the rate constants of decomplexation from 0.042 min^{-1} (1st cycle) to 0.073 min^{-1} (5th cycle). Cu(I) can not only reduce Fe(III), but it can also activate PDS [61]. It was worth noting that $^{\bullet}OH$ reacted with RH (alkyl groups of Fe-MOF) to produce alkyl radical ($R^{\bullet}$, Eq. 12) [62], which also accelerated the reduction of Fe(III) to Fe(II) (Eq. 13) [63]. The efficiency with which Cd-EDTA, Ni-EDTA, and Pd-EDTA were degraded by the EC/Fe-MOF/PDS system demonstrates its broad applicability. Unlike general organic pollutants such as antibiotics and pesticides, HMCs carry metal components. For synergistic effects, adding catalysts to stimulate self-catalyzed decomplexation is preferable. Testing various catalyst types, such as spinel and carbon materials, is worthwhile.

$$Fe^0 + 2S_2O_8^{2-} \rightarrow Fe^{2+} + 2SO_4^{\bullet-} + 2SO_4^{2-} \quad (9)$$

$$Ti_3C_2T_X + HSO_5^- \rightarrow \text{Oxidized-}Ti_3C_2T_X + SO_4^{\bullet-} + OH^- \quad (10)$$

$$Ti_3C_2T_X + HSO_5^- \rightarrow \text{Oxidized-}Ti_3C_2T_X + {}^{\bullet}OH + SO_4^{2-} \quad (11)$$

$$^{\bullet}OH + RH \rightarrow R^{\bullet} + H_2O \quad (12)$$

$$Fe^{3+} + R^{\bullet} \rightarrow Fe^{2+} + R^+ \quad (13)$$

3.3. Enhanced decomplexation by energy-transferring process

Activated PS energy transfer occurs *via* photolysis, pyrolysis, and ultrasound [64]. Ultraviolet (UV) is the most commonly used method for photolysis reactions. In the UV/PDS system, the entire decomplexation process of Cu-EDTA includes three stages (initial induction, quick decomplexation, and moderate decomplexation) [65]. The lower the dosage of PDS, the longer the induction

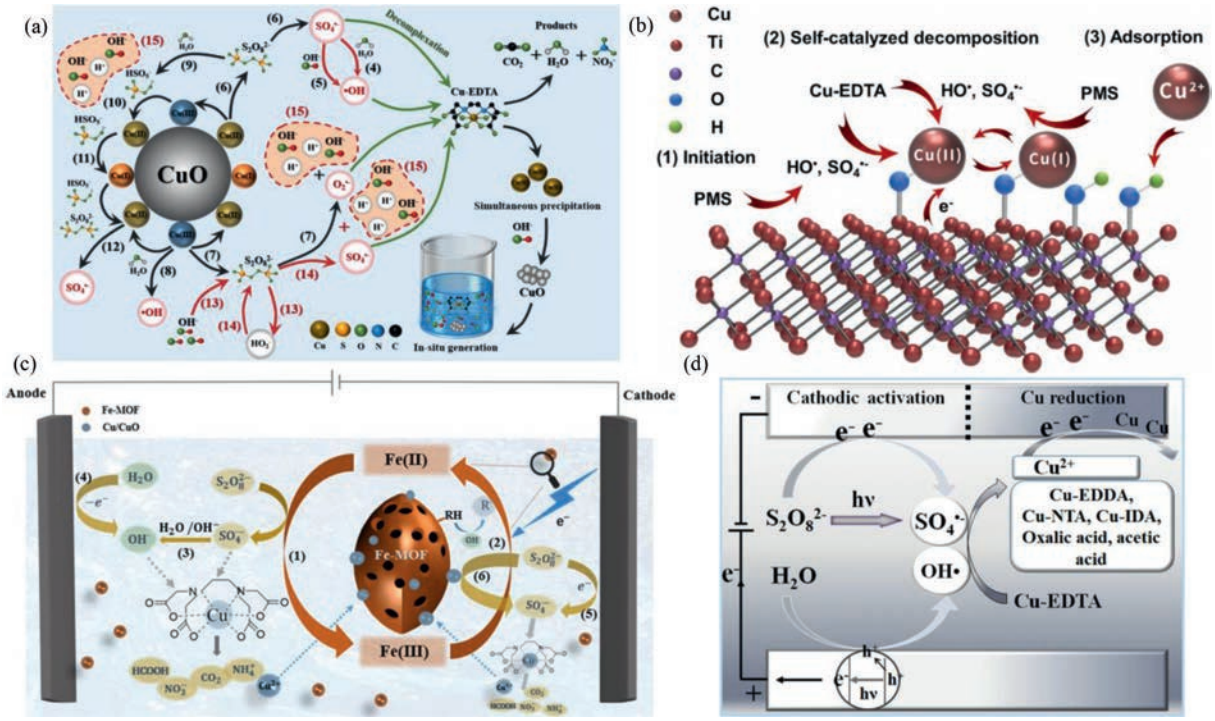

Fig. 3. (a) Possible activation mechanism for the synergistic activation of PS with Alkali and CuO. Reproduced with permission [50]. Copyright 2022, Elsevier. (b) Schematic diagram of the self-catalyzed decomplexation mechanism of Cu-EDTA in $Ti_3C_2T_x$/PMS process. Reproduced with permission [55]. Copyright 2022, Elsevier. (c) Proposed mechanism of Cu-EDTA degradation by EC/Fe-MOF/PS system. Reproduced with permission [59]. Copyright 2022, Elsevier. (d) Schematic of the PEC/$S_2O_8^{2-}$ process. Reproduced with permission [77]. Copyright 2016, American Chemical Society.

phase time. According to the EPR signal, the UV/PDS/Cu-EDTA system produced more $SO_4^{\bullet-}$ and $^{\bullet}OH$ than the UV/PDS system. Because Cu(I) in Cu-complexes was generated by the ligand-to-metal charge transfer (LMCT) process during the direct photolysis of UV irradiation [66]. Cu(I) then accelerated the decomposition of PDS. Before introducing PS in the reaction, the UV/H_2O_2 system was most frequently used. These two oxidants produced different ROS (Eqs. 14 and 15), with $SO_4^{\bullet-}$ being more selective than $^{\bullet}OH$ [67]. The removal of Cu-EDTA by the UV/PDS process was better than that by UV/H_2O_2 process under the same conditions. UV/PDS required a shorter induction time than UV/H_2O_2 at the same of oxidants. When the initial PDS dosage was 40 times greater than that of Cu(II)-EDTA, the induction stage lasted no more than 5 min. In contrast, the UV/H_2O_2 system needed around 90 min to stimulate the stage of fast decomplexation, even with H_2O_2 dosage 150 times higher than that of Cu(II)-EDTA. For TOC removal, the efficiency in the UV/H_2O_2 treatment system (<60%) was lower than that in the UV/PDS system (~90%) [68]. UV/PS and alkaline precipitation coupling could rapidly remove Cu-citrate and Cu-NTA. After the process, the concentration of Cu in the real electroplating effluent was deficient (<0.03 mg/L).

In the heat process, PDS was decomposed into two $SO_4^{\bullet-}$ (Eq. 16) [69]. Only 5.6% of Cu-EDTA was degraded under PDS conditions at 40 °C [70]. When the reaction temperature rose to 60 °C, the decomplexation efficiency reached 92.1%. The PDS conversion rate to $SO_4^{\bullet-}$ rapidly increased as the system temperature rose [71]. Meanwhile, the decomplexation of Cu-EDTA was remarkably enhanced with increasing the PDS dosage. Apart from the $SO_4^{\bullet-}$, $^1O_2$ and $^{\bullet}OH$ also participated in the degradation process. In the plating wastewater, various metals often coexist, including Cu(II), Ni(II), Cr(VI) [72]. The reduction of Cr(VI) has received limited attention. Adding formate (FA, $HCOO^-$) to the PDS system at 60–70 °C could oxidize Cu-EDTA and reduce Cr(VI). $SO_4^{\bullet-}$ and $^{\bullet}OH$ reacted with $HCOO^-$ to generate carbon dioxide anion radical ($CO_2^{\bullet-}$, Eqs. 17 and 18) [73]. $CO_2^{\bullet-}$ could efficiently reduce Cr(VI) to Cr(III) due to its low reduction potential (−1.9 V) [74]. If the concentration of FA was too low, Cr(VI) was converted into Cr(III) by excessive oxidation species in the later stage. When the FA dosage was high, the yield of oxidative free radicals decreased, thereby reducing the generation of $CO_2^{\bullet-}$ generation, which was not conducive to reducing Cr(VI). The optimum molar dosage of FA was half of PDS. The oxidation of Cu-EDTA and the reduction of Cr(VI) co-occurred, thus preventing the formation of Cr(III)-EDTA. Hydroxides, oxides, and carbonates of Cr(III) ($Cr(OH)_3$ and Cr_2O_3) and Cu(II) ($Cu(OH)_2$, CuO, $Cu_2CO_3(OH)_2$, and $CuCO_3$) were formed by the precipitation process. The advanced oxidation–reduction processes for plating wastewater treatment are worthy of in-depth research. There have been no reports on applying ultrasound-assisted PS for HMCs removal.

$$UV + S_2O_8^{2-} \rightarrow 2SO_4^{\bullet-} \quad (14)$$

$$UV + H_2O_2 \rightarrow 2^{\bullet}OH \quad (15)$$

$$Heat + S_2O_8^{2-} \rightarrow 2SO_4^{\bullet-} \quad (16)$$

$$SO_4^{\bullet-} + HCOO^- \rightarrow CO_2^{\bullet-} + SO_4^{2-} + H^+ \quad (17)$$

$$^{\bullet}OH + HCOO^- \rightarrow CO_2^{\bullet-} + H_2O \quad (18)$$

3.4. Coupling electron- and energy-transferring processes

To further accelerate the production of ROS in PS-based AOPs, coupling electron- and energy-transferring processes have been

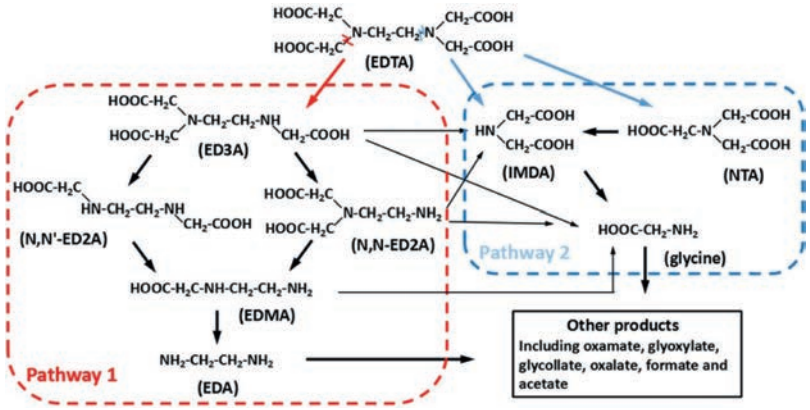

Fig. 4. Possible degradation pathway of EDTA summarized based on the available References. Reproduced with permission [65]. Copyright 2017, Elsevier.

utilized simultaneously to accelerate the production of ROS in PS-based AOPs [75]. Classical photo-electric synergistic catalysis is widely applied to AOPs [76]. Photo-electrocatalytic (PEC) PDS for the Cu-EDTA decomplexation and Cu recovery was reported by Zeng and co-workers [77]. Their results indicated that the decomplexation efficiency increased from 47.5% in the PEC system to 98.4% in the PEC/PDS system. However, almost no Cu-complexes were removed in the UV/PDS due to the conversion of Cu-EDTA to Cu-intermediates (NTA, ethylenediamine diacetate (EDDA), and iminodiacetic acid (IDA)). 21.6% of Cu-complexes were degraded in the EC/PDS system. Therefore, the synergism between EC and UV had significant advantages in activating PDS (Fig. 3d). The photoanode of TiO_2 in the PEC system mainly produced $^{\bullet}OH$ [78], which was different from the UV/PDS system. In addition to direct UV photolysis, the anode, and cathode could activate PDS [79,80]. In this PEC/PDS system, electrons originating from the cathode played a major role in the decomposition of PDS. The problem was the competition for electrons between the activation of PDS and the recycling of Cu. Compared to Cu(II) ions and Cu-EDTA, PDS tended to be preferentially reduced at the cathode according to the linear sweep voltammetry. During the initial 10 min, the cathode's surface exhibited minimal Cu deposition. However, after 45 min, a significant area was covered with a layer of Cu. Therefore, the rate of Cu recovery was slow in the early stage and increased in the later stage. Simultaneous HMCs decomplexation and metal ion recovery with multi-stage cascade reactors are promising possibilities [81]. Another coupling electron- and energy-transferring process to activate PDS was non-thermal plasma (NTP), which had a high electric field along with heat and UV irradiation [82]. In this system, the temperature could be maintained at about 35 °C. Various ROS including H_2O_2, O_3, $SO_4^{\bullet-}$, $^{\bullet}OH$, $O_2^{\bullet-}$, and $^1O_2$ were at play [83]. The NTP/PDS process produced more H_2O_2 and O_3 than the only NTP process. Quenching experiments of ROS indicated that $^1O_2$ was the crucial oxidizing species. After the Cu-EDTA decomplexation, the released Cu(II) ions also participated in the yield of ROS. Interestingly, the higher the operating voltage, the more Cu(II) ions were released [84]. 9.2%, 55.3%, and 86.0% of Cu-EDTA were degraded in the PDS, NTP, and NTP/PDS processes. With the operating voltage increase from 3.0 kV to 7.0 kV, the cooperative coefficient of NTP and PDS raised from 74.6 to 115. The higher PDS concentration or Cu(II)/EDTA ratio could enhance the decomplexation efficiency of Cu-EDTA. Cu was recovered from CuO, $Cu(OH)_2$, $Cu_2CO_3(OH)_2$, and $CuCO_3$ through an alkaline precipitation method. The Ni-EDTA degradation efficiency achieved about 90% in the NTP/PDS process, which showed it was an excellent option for HMCs removal. Many coupling processes must be developed and applied to remove HMCs, such as microwave/Fe(II)/PS, visible light/g-C_3N_4/PS, and ultrasound/ZVI/PS. Considerations of material savings and energy efficiency become crucial, as both electronic and energy transfers are promoted.

4. Decomplexation pathways of HMCs

In the PS-based AOPs, Cu-EDTA is the most representative HMCs (Table 2). EDTA is extensively researched due to its carboxyl group and C–N bond, and its interaction with heavy metals is intricate. Electroplating wastewater often contains Cu, a typical metal. As a result, our attention is directed towards understanding the decomplexation pathways of Cu-EDTA. There are two predominant decomplexation pathways of EDTA or metal-EDTA (Fig. 4) [65,85]. One is the successive decarboxylation process, and the other is that the C–N bond breaks first. In the UV/PDS system, Cu-NTA, Cu-IDA (or IMDA), and Cu-glycine were almost undetected. The concentrations of Cu-ED3A and Cu-ED2A (or EDDA) increased first and then decreased as the degradation time prolonged. Therefore, the continuous decarboxylation process was the chief decomplexation process. If *tert*–butyl alcohol quenching $^{\bullet}OH$, the generated byproducts were also Cu-ED3A and Cu-ED2A, which indicated that the successive decarboxylation process occurred in the $SO_4^{\bullet-}$-mediated AOPs. $SO_4^{\bullet-}$ belongs to electrophilic radicals, which preferentially attack electron-rich sites of organic pollutants [86]. Density functional theory (DFT) calculation can assist in analyzing degradation pathways [87]. For example, the Fukui index was applied to predict attack sites of Cu-EDTA [82]. The higher value of electrophilic attack (f^-), the stronger the activity of the site reacted with $SO_4^{\bullet-}$ [88]. The f^- value of the O site bonded to Cu was higher than that of the N site coordinated with Cu; thus, the decarboxylation process was more easily triggered. Once ROS were adequate, both carboxyl and amino processes were the main pathways. The pathway of the amino site involved cleaving the C–N bond in the -CH_2-CH_2-N- group of Cu-EDTA. IDA fell off, and the residue quickly oxidized to Cu-NTA by $^{\bullet}OH_2$. Subsequently, Cu-IDA was generated from Cu-NTA due to removing the carboxyl group [34]. Cu-EDDA was gradually oxidized to ethylene glycol, glycolic acid, dihydroxy, acetic acid, 1,4-butanediol, and 4-oxopentanoic. Cu-IDA was converted into glycine, oxamic acid, oxalic acid, and formic acid step by step [70]. The NH_4^+, NO_3^-, CO_2, and H_2O were also the byproducts indicating outstanding mineralization efficiency. The Cu(II) ions released after oxidation was recovered through alkali precipitation, adsorption, and electro-reduction, and membrane separation was less commonly used. For self-decomplexation of Ni-EDTA by PMS at Alkali, the major intermediate was ED3A, which was significantly more abundant than ED2A. And the TOC efficiency only achieved 19.1%. The Ni(IV)-mediated process was suitable for releasing Ni(II) ions and could not further oxidize the complexing agent [37]. Compared to degradation pathways by $SO_4^{\bullet-}$ and $^{\bullet}OH$

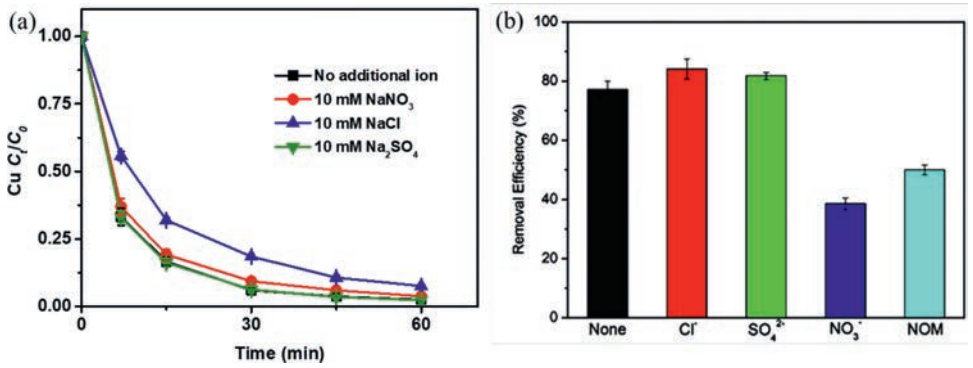

Fig. 5. (a) Effect of common anions on the decomplexation of Cu-EDTA by Co(II)/PMS process. Reproduced with permission [40]. Copyright 2020, Elsevier. (b) Effect of coexisting substances for removing EDTA-chelated Cu in the ZVI/PDS system. Reproduced with permission [47]. Copyright 2021, Elsevier.

oxidation, $^1O_2$-mediated decomplexation pathways may be different due to the addition $^1O_2$ to -C=C- [89], which required further study. The species proportion of metal-complexes varies under different pH values, which may influence decomplexation pathways. However, current research has overlooked this point. The decomplexation pathways of Co-EDTA, Cr-EDTA, and Pb-EDTA in PS-based AOPs are unclear.

It is necessary to evaluate the toxicity of degradation products. Because incomplete mineralization leads to the formation of highly toxic intermediates that pose a greater risk to the environment [90]. The toxicity of intermediates towards human hepatoellular carcinomas (HepG2) cells and luminescent bacteria in the UV/PDS/Cu-EDTA system was investigated by Wang and coworkers [68]. In most oxidation processes, the toxicity towards human HepG2 cells was reduced, but that towards luminescent bacteria was enhanced. When the ratio of Cu-EDTA and PDS was 1:10, the toxicity of the treated solution was the lowest. After applying UV/PDS oxidation, it was observed that precipitation had a marked impact on the reduction of toxicity. In comparison, the UV/H_2O_2 oxidation process received only modest influence from precipitation. After UV irradiation, the toxicity of EDTA-Cu may be altered by specific intermediary components. In addition to experiments, computer software (quantitative structure-activity relationship prediction by Toxicity Estimation Software Tool) simulation plays an auxiliary role in evaluating the toxicity of intermediates [91]. The degradation product toxicity of HMCs involves the interaction between organics and metals, and there are few reports on this aspect.

5. Effects of water environment constituents on HMCs decomplexation

The acidity and alkalinity of industrial wastewater containing HMCs fluctuate widely. For example, the pH value of electroplating wastewater ranges from 4 to 11 [92]. In general, PS-based AOPs could efficiently degrade HMCs under broad pH conditions. Because PS reduced the pH value, and $SO_4^{\bullet-}$ had a high oxidation potential [93]. In the self-catalyzed decomplexation process, acidity was beneficial for removing Cu-EDTA and Co-EDTA owing to the increased proportion of metal ions. However, Alkali was necessary for Ni-EDTA degradation due to the vital role of $[HO–Ni(II)-EDTA]^{3-}$. Besides coupling alkali activation, other electron-transferring processes operated at optimum pH 3–5. The initial pH had little effect on the EC/Fe-MOF/PDS system. However, the activity of ZVI decreased under alkaline conditions due to the formation of a passivation layer on its surface [94]. In the energy-transferring process, the decrease in the removal efficiency of HMCs was mainly attributed to the consumption of $SO_4^{\bullet-}$ by OH^- [95]. Considering the recovery of released metal ions under alkaline conditions, improving the adaptability of PS-based AOPs for decomplexation can reduce the dosage of reagents. In addition, the buffering capacity of actual wastewater may weaken the advantage of PS in reducing pH, and thus simulation experiments need to be close to the actual situation.

Numerous substances in the water environment affected the HMCs removal and byproduct formation in PS-based AOPs. These include chlorides, nitrates, carbonates/bicarbonates (CO_3^{2-}/HCO_3^-), sulfates, and NOM. Chloride ions (Cl^-) could convert into reactive chlorine species (RCS, chlorine (Cl_2), hypochlorous acid (HClO), chlorine radicals ($Cl^{\bullet}$), *etc.*) by PS, $SO_4^{\bullet-}$, and $^{\bullet}OH$ [96]. The presence of Cl^- could either facilitate or hinder the removal of contaminants, depending on the reactivity of the target substance. When RCS could attack the organics, Cl^- enhances the removal process. On the other hand, if the contaminant was degraded by RCS slowly, Cl^- consumes the oxidizing substances needed for effective degradation, resulting in an unsatisfactory treatment outcome [97]. Unfortunately, HMCs had a stable structure that could only be degraded by strong oxidizing agents, proving that Cl^- had adverse effects (Fig. 5a). However, in the ZVI/PDS system, Cl^- corroded ZVI, creating Fe(II) ions that indirectly activate PDS. This counteracted the inhibition effect of Cl^- and provided a way to prevent Cl^- from undermining PS-based AOPs (Fig. 5b). Nitrate ions (NO_3^-) influenced the removal of organics in a similar way as Cl^- [98]. $SO_4^{\bullet-}$ reacted with NO_3^- *via* electron transfer to generate SO_4^{2-} and nitrate radicals ($NO_3^{\bullet}$), resulting in the disappearance of $SO_4^{\bullet-}$. The oxidation ability of $NO_3^{\bullet}$ was lower than that of $SO_4^{\bullet-}$. Thus NO_3^- harmed the decomplexation of HMCs [47]. Sulfate ions (SO_4^{2-}) had little effect on the decomplexation process as it was a product of an activated PS reaction. The influence of CO_3^{2-}/HCO_3^- on the HMCs removal was more complicated, which differed from those of the above anions. In aquatic environments, both $SO_4^{\bullet-}$ and halogen radicals, for instance $Cl^{\bullet}$, could oxidize CO_3^{2-}/HCO_3^-, thus widely existing carbonate radicals ($CO_3^{\bullet-}$) in water [99]. It had a strong selective oxidation ability and rapidly degraded some specific organic pollutants, such as aniline [100]. For HMCs, $CO_3^{\bullet-}$ were difficult to oxidize. It was worth noting that PMS could be activated by HCO_3^- owing to its asymmetric peroxide bonds [101]. As for NOM, the quenching effect of some olefin organics and aromatic organics on $SO_4^{\bullet-}$ was stronger than that of aliphatic compounds [102]. NOM also could reduce metals [103], especially Cu(II) ions released in the Cu-EDTA decomplexation process. In addition, NOM, such as quinone compounds (*e.g.*, *p*-benzoquinone), also activated PS [104]. Although some of them are beneficial to the PS treatment of HMCs, most NOM still has a negative influence due to their quenching effect on radicals.

6. Conclusions and perspective

In this review, we have described the recent advances in using PS-based AOPs for HMCs decomplexation. We thoroughly discussed the characteristics of the two common oxidants (peroxymonosulfate (PMS) and peroxydisulfate (PDS)) that are used in PS-based AOPs and explained their crucial role in HMCs degradation. For the decomplexation mechanisms, self-catalyzed decomplexation processes, the electron-transferring process, energy transfers process, and coupling electron- and energy-transferring processes were responsible for HMCs degradation in PS-based AOPs. In the self-catalyzed decomplexation processes, the Co-EDTA/PMS and Cu-EDTA/PDS systems depended on $SO_4^{\bullet-}$ and $^{\bullet}OH$ under acidic or alkaline conditions. While in the Ni-EDTA/PMS system, Ni(IV) was the core species only at alkali conditions. In the electron-transferring process, homogeneous catalysis (Co(II)) and heterogeneous catalysis (ZVI, CuO, $Ti_3C_2T_X$, and Fe-MOF) were applied to improve decomplexation. The degradation efficiencies were improved due to faster self-decomplexation activation and more ROS generation. Photolysis and pyrolysis were used as energy transfers to accelerate the decomplexation of HMCs. Compared to Ni-EDTA, Cu-EDTA had a stronger UV light response. In coupling electron- and energy-transferring processes, more types of ROS ($O_2^{\bullet-}$, and $^1O_2$) participated in the decomplexation, except for $SO_4^{\bullet-}$ and $^{\bullet}OH$. Moreover, the decomplexation mainly had two pathways: carboxyl and amino processes. Based on PS-based AOPs, the successive decarboxylation process occurred preferentially. The Ni(IV)-mediated decomplexation process only released Ni(II) ions, but complete mineralization of the complexing agent is difficult. The impact of water environmental environment conditions (pH, inorganic ions, and NOM) was also emphasized. Most PS-based AOPs had excellent degradation performance for decomposing HMCs under neutral-alkaline conditions. Low pH values could improve removal efficiency, except for the typical self-activation system of Ni-EDTA/PMS. $SO_4^{\bullet-}$ reacted with Cl^-, NO^{3-}, and CO_3^{2-}/HCO_3^-, to generate RCS, $NO_3^{\bullet}$, and $CO_3^{\bullet-}$, respectively. However, the effectiveness of RCS, $NO_3^{\bullet}$, and $CO_3^{\bullet-}$ attacking HMCs deteriorated. Although some NOM could activate PS, most of them compete with HMCs for ROS.

Overall, HMCs removal by PS-based AOPs research is growing rapidly, and there has already been significant advance, but some challenge is still ahead. We hope that future research is needed to consider the following suggestions:

(1) The self-catalyzed decomplexation mechanisms of various HMCs differ greatly due to the differences in metal electron distribution and coordination modes and the structural differences between PMS and PDS. Approximately 85% of the reported papers focus on Cu-EDTA decomplexation. Except for Co-EDTA, Cu-EDTA, and Ni-EDTA, other HMCs should be studied.
(2) Heterogeneous catalysts are essential in electron-transferring processes that improve decomplexation. Reducing the energy barrier of HMCs for self-decomplexation by utilizing the characteristics of the material is a good choice, but it is necessary to improve the adsorption performance of the catalyst to enhance electron transfer.

In the energy-transferring processes, the activation of PS by ultrasound for HMCs removal has received little attention. And there are few reports on the activation of PMS by energy.

(1) It is necessary to simultaneously consider the decomplexation of HMCs and the recovery of released metal ions. Cheap, easy-to-operate, and environmentally-friendly coupling processes should be designed.
(2) The radical-based decomplexation pathways are relatively explicit, but the non-radical mediated degradation process has not been explained clearly.
(3) The coexistence of different HMCs in actual industrial wastewater necessitates selective oxidation in PS-based AOPs and step-by-step metal recovery.

Declaration of competing interest

The authors declare that they have no known competing financial interests or personal relationships that could have appeared to influence the work reported in this paper.

Acknowledgments

This work was financially supported by National Natural Science Foundation of China (Nos. U22A20403, 22006047), Natural Science Foundation of Hebei Province (Nos. E2021203140, B2021203016), Hebei Industrial Innovation and Entrepreneurship team (No. 215A7608D).

References

[1] S. Chowdhury, M.A.J. Mazumder, O. Al-Attas, et al., Sci. Total Environ. 569-570 (2016) 476–488.
[2] W. Gao, M. Roger Razanajatovo, Y. Song, et al., Chem. Eng. J. 429 (2022) 132599.
[3] Q. Huang, Y. Zhang, W. Zhou, et al., Chin. Chem. Lett. 32 (2021) 2797–2802.
[4] W. Zhang, Q. Li, R. Li, et al., Sep. Purif. Technol. 282 (2022) 120151.
[5] J. Zhang, J. Luo, X. Zhao, et al., J. Environ. Sci. 126 (2023) 198–210.
[6] W. Liu, Y. Yu, Environ. Technol. Innov. 23 (2021) 101644.
[7] Z. Xu, Q. Zhang, X. Li, et al., Chem. Eng. J. 429 (2022) 131688.
[8] X.W. Zhang, M.Y. Lan, F. Wang, et al., Chem. Eng. J. 450 (2022) 138082.
[9] X. Du, M.A. Oturan, M. Zhou, et al., Appl. Catal. B: Environ. 296 (2021) 120332.
[10] S. He, T. Li, L. Zhang, et al., Chem. Eng. J. 424 (2021) 130515.
[11] J. Du, B. Zhang, J. Li, et al., Chin. Chem. Lett. 31 (2020) 2575–2582.
[12] Y. Zhu, W. Fan, W. Feng, et al., J. Hazard. Mater. 414 (2021) 125517.
[13] Q. Zhang, X. Wang, J. Xie, et al., J. Hazard. Mater. 443 (2023) 130280.
[14] X. Li, F. Ye, H. Zhang, et al., J. Environ. Chem. Eng. 11 (2023) 110329.
[15] F. Deng, H. Olvera-Vargas, M. Zhou, et al., Chem. Rev. 123 (2023) 4635–4662.
[16] W. Guan, B. Zhang, S. Tian, et al., Appl. Catal. B: Environ. 227 (2018) 252–257.
[17] C. Chen, P. Liu, Y. Li, et al., Water Res. 218 (2022) 118502.
[18] D. Ma, H. Yi, C. Lai, et al., Chemosphere 275 (2021) 130104.
[19] M.N. Arifin, R. Jusoh, H. Abdullah, et al., Environ. Res. 229 (2023) 115936.
[20] C. Dong, W. Fang, Q. Yi, et al., Chemosphere 308 (2022) 136205.
[21] M. Li, Z. He, H. Zhong, et al., Water Res. 200 (2021) 117266.
[22] F. Ghanbari, M. Moradi, Chem. Eng. J. 310 (2017) 41–62.
[23] S. Wacławek, H.V. Lutze, K. Grübel, et al., Chem. Eng. J. 330 (2017) 44–62.
[24] X. Wu, J.H. Kim, ACS ES&T Eng. 2 (2022) 1776–1796.
[25] Q. Yang, Y. Ma, F. Chen, et al., Chem. Eng. J. 378 (2019) 122149.
[26] W.D. Oh, Z. Dong, T.T. Lim, Appl. Catal. B: Environ. 194 (2016) 169–201.
[27] J. Lee, U. von Gunten, J.H. Kim, Environ. Sci. Technol. 54 (2020) 3064–3081.
[28] J. Wang, S. Wang, Chem. Eng. J. 334 (2018) 1502–1517.
[29] X. He, A.A. de la Cruz, D.D. Dionysiou, J. Photochem. Photobiol. A: Chem. 251 (2013) 160–166.
[30] S. Giannakis, K.Y.A. Lin, F. Ghanbari, Chem. Eng. J. 406 (2021) 127083.
[31] J. Lee, B.K. Singh, M.A. Hafeez, et al., Chemosphere 300 (2022) 134494.
[32] X. Du, M. Zhou, Chem. Eng. J. 403 (2021) 126346.
[33] X.H. Yi, H. Ji, C.C. Wang, et al., Appl. Catal. B: Environ. 293 (2021) 120229.
[34] Q. Wang, Y. Li, Y. Liu, et al., J. Clean. Prod. 314 (2021) 128119.
[35] B. Liu, Y. Li, Y. Wu, et al., Chem. Eng. J. 417 (2021) 127972.
[36] T. Wang, Y. Cao, G. Qu, et al., Environ. Sci. Technol. 52 (2018) 7884–7891.
[37] S. Liang, X. Hu, H. Xu, et al., Appl. Catal. B: Environ. 296 (2021) 120375.
[38] X. Wang, Z. Xiong, H. Shi, et al., Appl. Catal. B: Environ. 329 (2023) 122569.
[39] J. Qi, X. Yang, P.Y. Pan, et al., Environ. Sci. Technol. 56 (2022) 5200–5212.
[40] Z. Xu, T. Wu, Y. Cao, et al., Chem. Eng. J. 392 (2020) 123639.
[41] J. Qi, J. Liu, F. Sun, et al., Chin. Chem. Lett. 32 (2021) 1814–1818.
[42] Y. Zhu, W. Fan, T. Zhou, et al., Sci. Total Environ. 678 (2019) 253–266.
[43] X. Guan, X. Jiang, J. Qiao, et al., J. Hazard. Mater. 300 (2015) 688–694.
[44] Z. Xu, G. Gao, B. Pan, et al., Water Res. 87 (2015) 378–384.
[45] S. Yang, Y. Xue, M. Wang, Prog. Chem. 31 (2019) 1187–1198.
[46] M. Liao, S. Zhao, K. Wei, et al., Appl. Catal. B: Environ. 330 (2023) 122619.
[47] L. Fei, S. Ren, M. Xijun, et al., Sep. Purif. Technol. 279 (2021) 119721.
[48] X. Li, Y. Qin, Y. Jia, et al., Chemosphere 274 (2021) 129766.
[49] C. Ling, S. Wu, J. Han, et al., Water Res. 220 (2022) 118676.
[50] Y. Hong, Z. Luo, N. Zhang, et al., Sci. Total Environ. 817 (2022) 152793.
[51] S. Xing, W. Li, B. Liu, et al., Chem. Eng. J. 382 (2020) 122837.
[52] J. Jing, X. Wang, M. Zhou, Water Res. 232 (2023) 119682.
[53] W. Li, W. Li, K. He, et al., J. Hazard. Mater. 432 (2022) 128719.
[54] Z. Xiong, Y. Jiang, Z. Wu, et al., Chem. Eng. J. 421 (2021) 127863.
[55] D. Zu, H. Song, C. Li, et al., Appl. Catal. B: Environ. 306 (2022) 121131.
[56] C. Wang, J. Ye, L. Liang, et al., Sci. Total Environ. 862 (2023) 160539.
[57] Q. Zhou, P. Hong, X. Shi, et al., J. Hazard. Mater. 448 (2023) 130995.
[58] P. Su, W. Fu, Z. Hu, et al., Appl. Catal. B: Environ. 313 (2022) 121457.

[59] Y. Zhang, J. Sun, Z. Guo, et al., Chem. Eng. J. 430 (2022) 133025.
[60] X. Wang, Q. Zhang, J. Jing, et al., Chem. Eng. J. 466 (2023) 143283.
[61] X. Du, W. Fu, P. Su, et al., ACS ES&T Eng. 1 (2021) 1311–1322.
[62] J. Wang, S. Wang, Chem. Eng. J. 401 (2020) 126158.
[63] X. Wang, J. Jing, M. Zhou, et al., Chin. Chem. Lett. 34 (2023) 107621.
[64] U. Ushani, X. Lu, J. Wang, et al., Chem. Eng. J. 402 (2020) 126232.
[65] Z. Xu, C. Shan, B. Xie, et al., Appl. Catal. B: Environ. 200 (2017) 439–447.
[66] X. Huang, Y. Wang, X. Li, et al., Environ. Sci. Technol. 53 (2019) 2036–2044.
[67] Z. Yang, J. Qian, C. Shan, et al., Environ. Sci. Technol. 55 (2021) 14494–14514.
[68] Y. Wang, Y. Liu, B. Wu, et al., Chemosphere 240 (2020) 124942.
[69] W. Ren, X. Huang, L. Wang, et al., Chem. Eng. J. 426 (2021) 131876.
[70] Q. Wang, Y. Zhang, Y. Li, et al., Chem. Eng. J. 427 (2022) 131584.
[71] K. Zhang, D. Sun, C. Ma, et al., Chemosphere 241 (2020) 125021.
[72] F. Zeng, C. Chen, X. Huang, Chemosphere 241 (2020) 125124.
[73] H. Ren, Z. Hou, X. Han, et al., Chem. Eng. J. 309 (2017) 638–645.
[74] C.M. Hendy, G.C. Smith, Z. Xu, et al., J. Am. Chem. Soc. 143 (2021) 8987–8992.
[75] K. Tian, L. Hu, L. Li, et al., Chin. Chem. Lett. 33 (2022) 4461–4477.
[76] H. Wu, Z. Hu, R. Liang, et al., Appl. Catal. B: Environ. 321 (2023) 122053.
[77] H. Zeng, S. Liu, B. Chai, et al., Environ. Sci. Technol. 50 (2016) 6459–6466.
[78] X. Zhao, L. Guo, B. Zhang, et al., Environ. Sci. Technol. 47 (2013) 4480–4488.
[79] J. Cai, M. Zhou, Q. Zhang, et al., J. Hazard. Mater. 416 (2021) 125804.
[80] L. Bu, J. Ding, N. Zhu, et al., Appl. Catal. B: Environ. 253 (2019) 140–148.
[81] Y. Liu, G. Gao, C.D. Vecitis, Acc. Chem. Res. 53 (2020) 2892–2902.
[82] Y. Liu, G. Qu, Q. Sun, et al., Chem. Eng. J. 406 (2021) 126774.
[83] F. Saleem, J. Harris, K. Zhang, et al., Chem. Eng. J. 382 (2020) 122761.
[84] Q. Wang, J. Yu, X. Chen, et al., J. Environ. Manage. 248 (2019) 109237.
[85] M. Li, N. Chen, H. Shang, et al., Environ. Sci. Technol. 56 (2022) 10945–10953.
[86] L. Chen, H. Ji, J. Qi, et al., Chem. Eng. J. 406 (2021) 126877.
[87] Y. Li, Y. Yang, J. Lei, et al., Sci. Total Environ. 779 (2021) 146498.
[88] F.X. Wang, Z.C. Zhang, C.C. Wang, Chem. Eng. J. 459 (2023) 141538.
[89] B. Barrios, B. Mohrhardt, P.V. Doskey, et al., Environ. Sci. Technol. 55 (2021) 8054–8067.
[90] X. Liu, G. Liu, S. Liu, et al., J. Hazard. Mater. 443 (2023) 130367.
[91] T. Wang, C. Zhao, L. Meng, et al., Appl. Catal. B: Environ. 334 (2023) 122832.
[92] X. Tao, X. Hu, Z. Wen, et al., J. Hazard. Mater. 424 (2022) 127423.
[93] J. Wang, B. Li, Y. Li, et al., ACS Appl. Mater. Interfaces 13 (2021) 2630–2641.
[94] W. Xiang, X. Zou, M. Huang, et al., J. Environ. Chem. Eng. 10 (2022) 107547.
[95] D. Jiang, D. Fang, Y. Zhou, et al., Environ. Pollut. 306 (2022) 119386.
[96] W. Peng, Y. Fu, L. Wang, et al., Chin. Chem. Lett. 32 (2021) 2544–2550.
[97] K. Guo, Z. Wu, C. Chen, et al., Acc. Chem. Res. 55 (2022) 286–297.
[98] C. Yu, Z. Xiong, H. Zhou, et al., Chem. Eng. J. 433 (2022) 133802.
[99] L. Lian, B. Yao, S. Hou, et al., Environ. Sci. Technol. 51 (2017) 2954–2962.
[100] L. Carena, D. Vione, M. Minella, et al., Water Res. 209 (2022) 117867.
[101] A. Kottapurath Vijay, V. Marks, A. Mizrahi, et al., Environ. Sci. Technol. 57 (2023) 6743–6753.
[102] L. Varanasi, E. Coscarelli, M. Khaksari, et al., Water Res. 135 (2018) 22–30.
[103] J. Adusei-Gyamfi, B. Ouddane, L. Rietveld, et al., Water Res. 160 (2019) 130–147.
[104] Y. Wang, J.Le Roux, T. Zhang, et al., Environ. Sci. Technol. 48 (2014) 14534–14542.